



Noise Analysis of Strong Motion and Microtremor Observation Records for Soil-Building Structure Dynamic Interaction

T. Azuhata⁽¹⁾, H. Okano⁽²⁾, M. Yasui⁽³⁾, M. Iiba⁽⁴⁾, N. Inoue⁽⁵⁾, T. Tanuma⁽⁶⁾

⁽¹⁾ Chief Research Engineer, IISEE, Building Research Institute, azuhata@kenken.go.jp

⁽²⁾ Professor, Chiba University, hajimeokano@chiba-u.jp

⁽³⁾ Section Chief, Toda Corporation, mitoshi.yasui@toda.co.jp

⁽⁴⁾ Professor, Hokkaido University, iiba-m@eng.hokudai.ac.jp

⁽⁵⁾ Chief Research Engineer, Building Research Institute, inoue_n@kenken.go.jp

⁽⁶⁾ Senior Research Engineer, Building Research Institute, t-tanuma@kenken.go.jp

Abstract

Dynamic soil-structure interaction largely affects the seismic performance of building structures in many cases. It is effective to measure real behaviors of a building and the surrounding ground with seismographs to explain this effect. Some previous studies detected the SSI effects to system parameters such as natural frequencies and damping coefficients by using Fourier spectrum ratios to evaluate earthquake response characteristics of building structures. The Fourier spectrum ratios calculated from observation records correspond to transfer functions from input motions to responses. However, they have different features from the general transfer functions in actuality. They are not smooth and include some noises. In this study, we investigate characteristics of these noises included in microtremor and strong motion observation records and generation factors of them.

The target building in this study is a five-story apartment with a reinforced concrete wall structural system. The dimension of its plan is 65.7m by 6.96m. The height is 26.7m. We arranged sensors for microtremor and strong motion observation at multi-points in this building. For the microtremor observation, we also set sensors at the multi-points on the surrounding ground. On the other hand, we set only one sensor at the single-point on it for the strong motion observation. We acquired records of three directional motions. However, this paper deals with records in only a long-span direction of the building.

Analysis results of microtremor observation records showed that coherence between ground motions observed near both edges of the building decreased in a higher frequency range and became almost zero in the range higher than 2Hz. It means that there were significant phase differences between ground motions input to the both edges of the building structure especially in the range of high frequency. In contrast, the coherences among records observed in the building became higher than that of ground motions. Based on these results, we can presume that the rigidity of the floors in the building probably has a particular effect decreasing noises included in the observation records. Using observed ground motions, we execute numerical analyses and examine effects of floor rigidities to noises appeared in the Fourier response spectral ratios.

Also, we analyze noises included in microtremor and strong motion observation records using the signal power ratio proposed by Ikeura.

From the results of this study, we concluded that flexible floors of the building with a long span tend to generate larger noises on the Fourier spectral ratios, and we can evaluate more appropriate transfer functions from observation records with considering the signal power ratio.

Keywords: Coherence; Microtremor observation; Strong motion observation; Fourier spectral ratio; Transfer function.



1. Introduction

Dynamic soil-structure interaction (SSI) largely affects the seismic performance of building structures in many cases. It is effective to measure real behaviors of a building and the surrounding ground with seismographs to clear this effect as shown by the previous works [e.g., 1-6]. Some of them detected the SSI effects to system parameters such as natural frequencies and damping factors by using Fourier spectrum ratios to evaluate earthquake response characteristics of the buildings. The Fourier spectrum ratios calculated from observation records correspond to transfer functions from input motions to responses. However, they have different features from the general transfer functions in actuality. They are not smooth and include some noises. In this study, we investigate characteristics of these noises and generation factors of them.

2. Records of Microtremor and Strong Motion Observation

2.1 Target building structure for observation

Photo 1 shows the building structure targeted in this study. The target building is a five-story apartment with a reinforced concrete wall structural system. The dimension of the plan is 65.7m by 6.96m. The height is 26.7m. The building has no basement and 126 PC piles of which length is 20m and diameter is 300mm. Table 1 shows the structure of surface ground around the target building.



Photo 1 - Target building

Table - 1 Structure of surface ground

| Layer thickness (m) | Shear wave velocity (m/s) | Density (t/m ³) | Soil property |
|---------------------|---------------------------|-----------------------------|---------------|
| 3.0 | 80-110 | 1.6 | Silt |
| 4.7 | 150 | 1.8 | Fine sand |
| 7.65 | 190-230 | 1.8 | Fine sand |
| 7.9 | 270-390 | 1.8 | Fine sand |
| 2.55 | 270 | 1.7 | Silt |
| 6.9 | 380 | 1.8 | Fine sand |
| - | 540 | 1.8 | Fine sand |

Table 2 - System parameters of target building

| | |
|--|------------------|
| Mass of superstructure, $3m_s$ | 3038 (t) |
| Mass of base, $3m_b$ | 1523 (t) |
| Shear stiffness of superstructure, $3k_s$ | 4.06e+06 (kN/m) |
| Damping ratio of superstructure | 0.065 |
| Stiffness of sway soil spring, $3k_{sway}$ | 1.53e+06 (kN/m) |
| Damping of sway soil spring, $3c_{sway}$ | 2.40e+04 (kNs/m) |



We can estimate the mass of the superstructure and the foundation from the drawing. Furthermore, the previous research by part of us identified shear stiffness and damping factor of the superstructure, and complex stiffness of sway soil springs using strong motion observation records which are also employed for this study [6]. Table 2 shows these values.

2.2 Microtremor observation

We conducted microtremor observation on Feb. 5 in 2011. Fig.1 shows the sensor arrangement for microtremor observation in the long-span direction. We also observed a behavior of the structure in the short-span direction with the different sensor arrangement. However, this study deals with only the long-span direction. Fig.2 shows a velocity time history observed at GL(1) in Fig.1 as an example of observation records. This study targets records in 100-300s. Fig.3 shows Fourier spectral ratios calculated with records at GL(1), 1F(4) and RF(7). And Fig.4 shows coherences, coh^2 , of GL(1) vs. GL(3), 1F(4) vs. 1F(6) and RF(7) vs. RF(9).

The following equation defines the coherence.

$$coh^2(f) = \frac{C_{xy}(f)C_{xy}(f)^*}{C_{xx}(f)C_{yy}(f)} \quad (1)$$

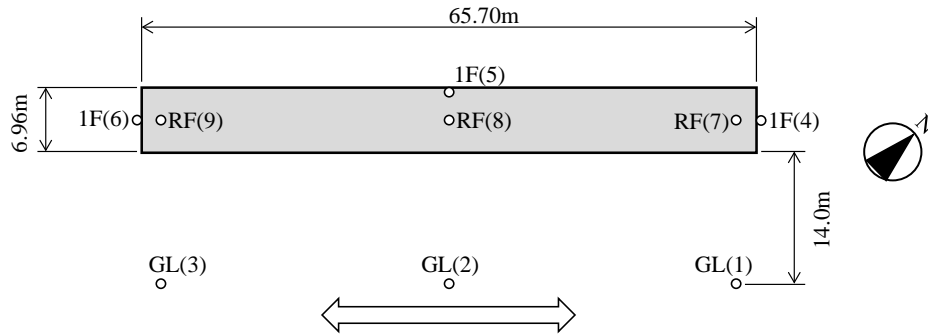


Fig.1 - Sensor arrangement for microtremor observation

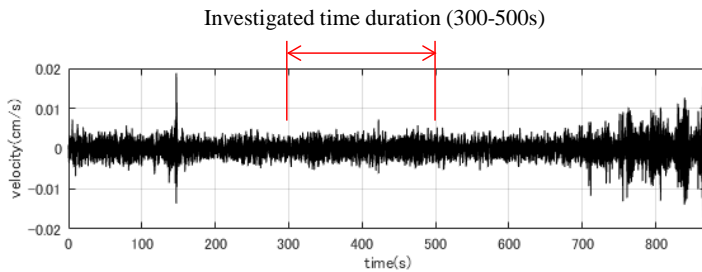


Fig.2 - Microtremor observation record on GL(1)

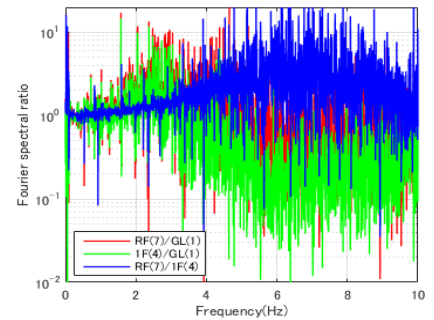


Fig.3 - Fourier spectral ratios of microtremor records

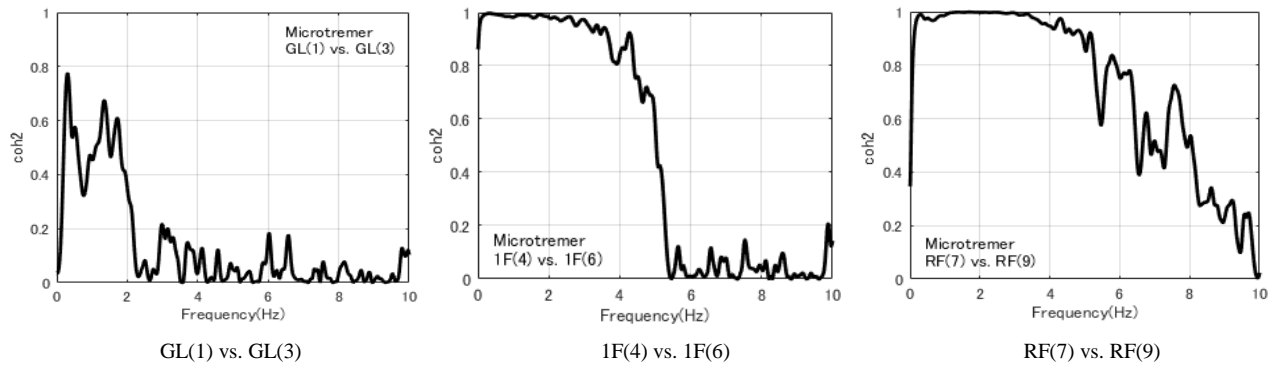


Fig.4 - Coherence, coh^2 , of microtremor records

Where, $C_{xy}(f)$: cross spectrum, $C_{xx}(f)$ and $C_{yy}(f)$: power spectra.

In this study, we apply Eq.(1) using cross spectrum and power spectra smoothed with a spectral window of which bandwidth is 0.2Hz instead of ensemble averages of them. These smoothed spectra can be acquired from only one set of records.

Fig.4 shows that coherence between GL(1) and GL(3) becomes almost zero in the range where the frequency is higher than 2Hz. It means that phase difference between ground motions are apparently large in this range. On the other hand, a coherence of 1F(4) vs. 1F(6) and that of RF(7) vs. RF(9) are higher than that of ground motions. At the point where the frequency is about 4Hz, coherences of structure responses are almost 1.0 although coherence of ground motions observed near the both edges of the structure, which are GL(1) and GL(3), is almost 0.0. We can presume that the both edges of the structure show the similar behavior due to an effect of floor rigidity even if ground moves independently.

2.3 Strong motion observation

We started strong motion observation on Feb. 5 in 2011 and continue it even now. Fig.5 shows the sensor arrangement for strong motion observation. In this study, we analyze records observed on Apr. 11 in 2011. Fig.6 shows acceleration time history observed at GL(1). We analyze the records in the time range of 60-100s.

Fig.7 shows Fourier spectral ratios. There are some noises on them. However, they are smoother than those shown in Fig.3. Fig.8 shows coherences, coh^2 , calculated with strong motion observation records. The coherence between 1F(2) and 1F(4) tends to decrease in the range higher than about 4Hz. However, the coherences for the strong motion are superior to those for the microtremor.

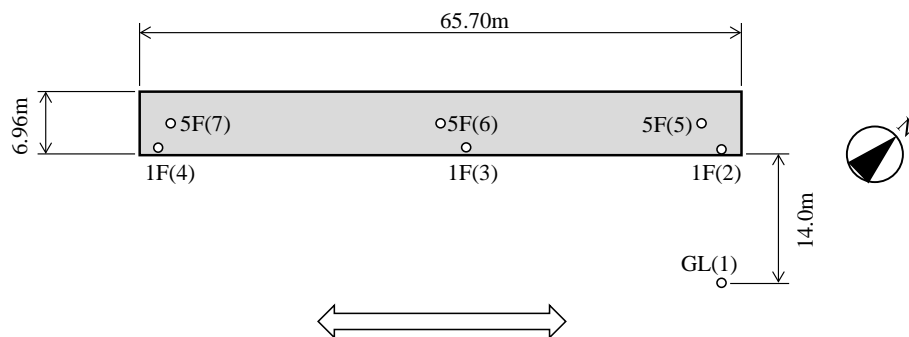


Fig.5 - Sensor arrangement for strong motion observation

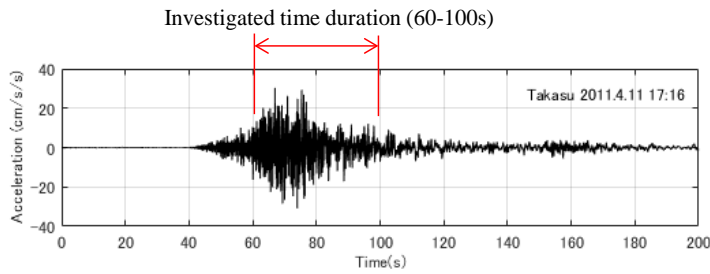


Fig.6 - Strong motion observation record on GL(1)

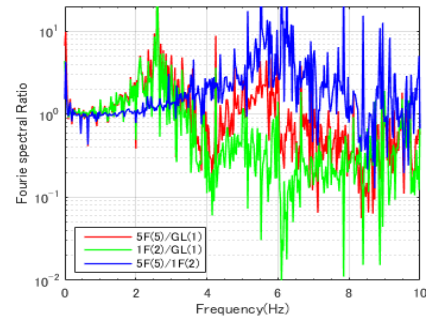


Fig.7 - Fourier spectral ratios of strong motion records

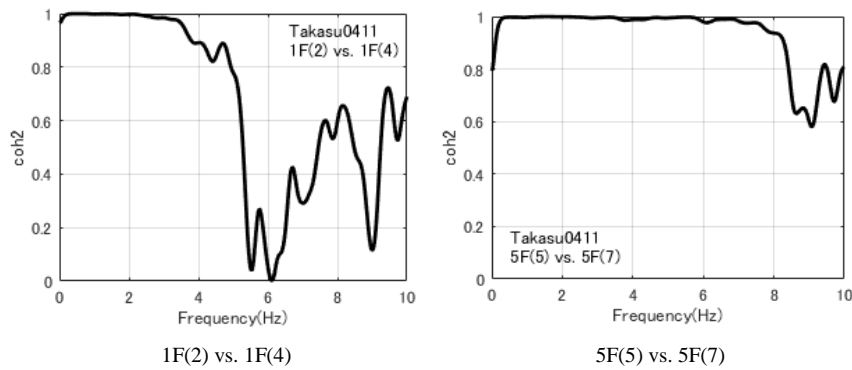


Fig. 8 - Coherence, coh^2 , of strong motion observation records

3. Effects of Floor Rigidities in Microtremor Observation Records

We make a numerical model shown in Fig.9 for investigating effects of floor rigidities.

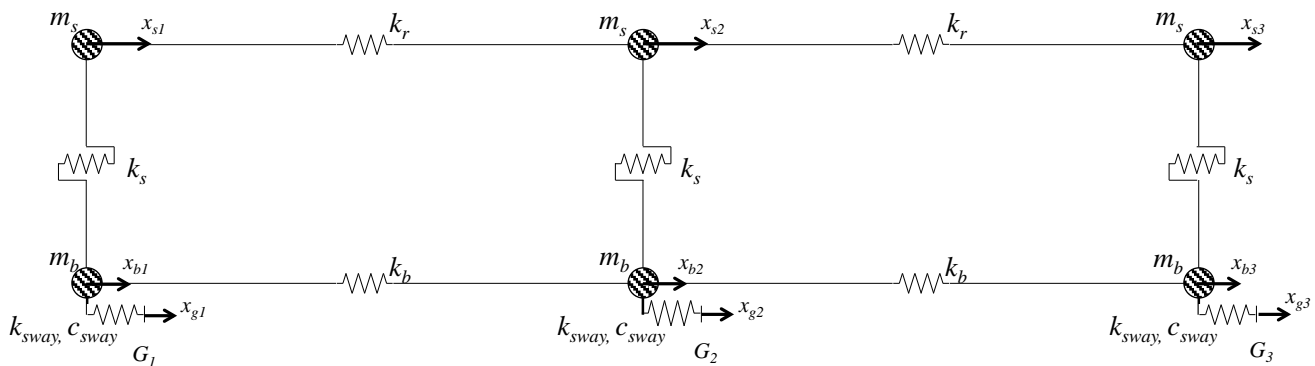


Fig.9 - Numerical model for investigating effects of floor rigidities (k_b & k_r)

Eq. (2) expresses the equation of motion in the frequency domain for this model.



$$\left\{ -\omega^2 \begin{bmatrix} [M_{ss}] & 0 \\ 0 & [M_{bb}] \end{bmatrix} + \begin{bmatrix} [K_{ss}] + i\omega[C_{ss}] & [K_{rb}] + i\omega[C_{sb}] \\ [K_{bs}] + i\omega[C_{bs}] & [K_{bb}] + i\omega[C_{bb}] \end{bmatrix} \right\} \begin{Bmatrix} X_s \\ X_b \end{Bmatrix} = \begin{Bmatrix} 0 \\ P \end{Bmatrix} \quad (2)$$

Where, X_s : displacements of superstructure, $\{x_{s1}, x_{s2}, x_{s3}\}^T$, X_b : displacements of basement, $\{x_{b1}, x_{b2}, x_{b3}\}^T$, P : driving force which is calculated by the following equation.

$$P = (k_{sway} + i\omega c_{sway}) [I] X_g = [K_{soil}] X_g \quad (3)$$

Where, $[I]$: unit matrix, X_g : displacements of soil at the points denoted by $G_{1,2,3}$ in Fig.9, $\{x_{g1}, x_{g2}, x_{g3}\}^T$. In Eq.(2), $[K_{bb}]$ and $[C_{bb}]$ contain k_{sway} and c_{sway} respectively.

Let us separate displacement X in Eq.(2) as shown in the following.

$$\begin{Bmatrix} X_s \\ X_b \end{Bmatrix} = \begin{Bmatrix} X_s^s \\ X_b^s \end{Bmatrix} + \begin{Bmatrix} X_s^d \\ X_b^d \end{Bmatrix} \quad (4)$$

The vectors, X_s^s and X_b^s , in Eq. (4) should satisfy the following condition. It reveals equilibrium of force under the assumption that mass equals to zero.

$$\begin{bmatrix} K_{ss} + i\omega C_{ss} & K_{sb} + i\omega C_{sb} \\ K_{bs} + i\omega C_{bs} & K_{bb} + i\omega C_{bb} \end{bmatrix} \begin{Bmatrix} X_s^s \\ X_b^s \end{Bmatrix} = \begin{Bmatrix} 0 \\ P \end{Bmatrix} \quad (5)$$

The following equation can be derived substituting Eq. (4) into Eq. (2), with considering Eq. (3) and Eq. (5).

$$\left\{ -\omega^2 [M] + [K] \right\} \begin{Bmatrix} X_s^d \\ X_b^d \end{Bmatrix} = \omega^2 [M] [K]^{-1} \begin{Bmatrix} [0] \\ [K_{soil}] \end{Bmatrix} X_g \quad (6)$$

Where, $[M]$: mass matrix and $[K]$: stiffness matrix.

The matrices $[M]$ $[K]$ and $[K_{soil}]$ consists of values shown in Table 2.

If all elements in the vector X_g are the same, thus $x_{g1}=x_{g2}=x_{g3}=x_g$, the right side of Eq. (6) can be expressed by Eq. (7) as it is well-known.

$$\omega^2 [M] [K]^{-1} \begin{Bmatrix} [0] \\ [K_{soil}] \end{Bmatrix} X_g = \omega^2 [M] \{1\} x_g \quad (7)$$

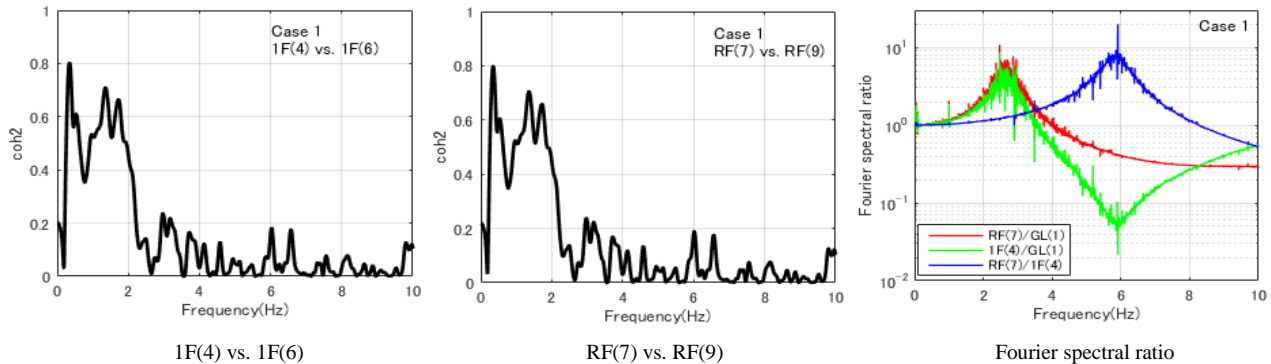


Fig.10 - Coherence and Fourier spectral ratio (case 1: $k_b=0.01k_s$, $k_r=0.01k_s$)

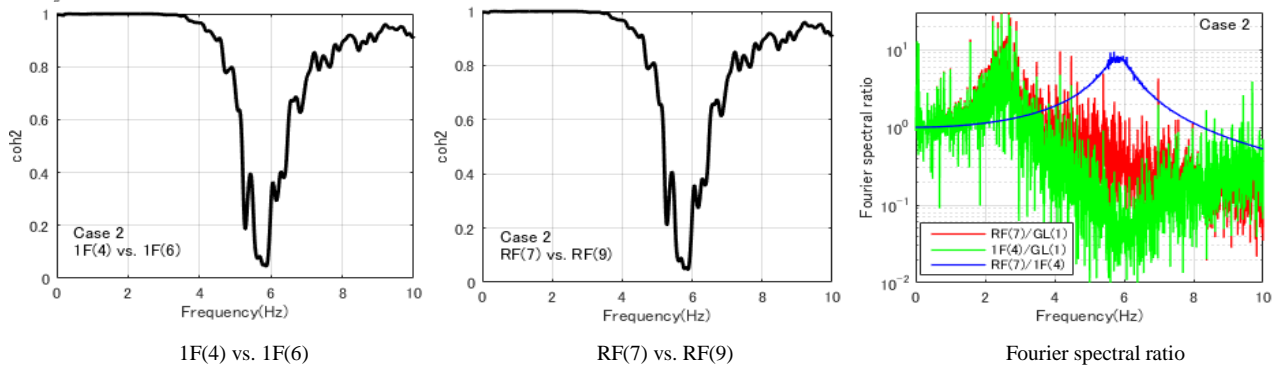


Fig.11 - Coherence and Fourier spectral ratio (case 2: $k_b=10k_s$, $k_r=0.01k_s$)

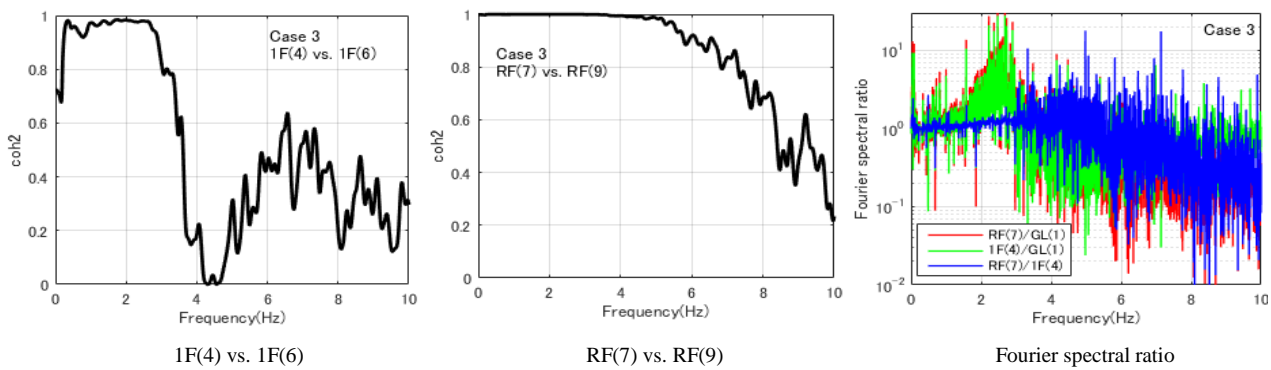


Fig.12 - Coherence and Fourier spectral ratio (case 3: $k_b=0.01k_s$, $k_r=10k_s$)

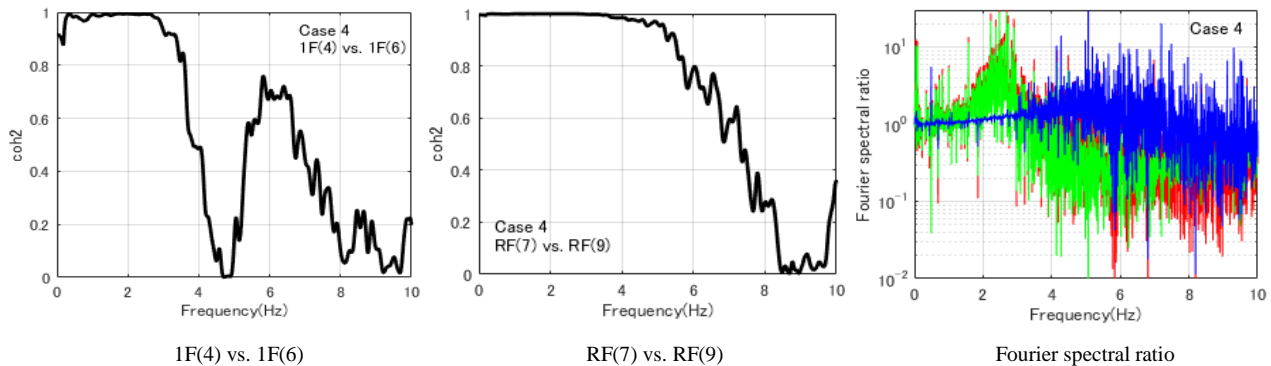


Fig.13 - Coherence and Fourier spectral ratio (case 4: $k_b=1.096k_s$, $k_r=3.281k_s$)

To investigate effects of floor rigidities to microtremor observation records, we carry out parametric studies using the numerical model shown in Fig.9. In this parametric studies, the microtremor records observed at the ground points, which are GL(1), GL(2) and GL(3), are used as input motions. Substituting these three microtremor observation records on the ground into X_g of Eq. (3) and solving Eq. (2), we can estimate response value X_f at any point. Fig.10 shows coherences, coh^2 , and Fourier spectral ratios of the numerical model of which both rigidities of bases and roofs, k_b and k_r , are set to 0.01 times of shear stiffness, k_s . Fig.11 shows the results of the case where rigidities of only the bases, k_b , in the numerical model are increased to ten times of shear stiffness k_s . In contrast, Fig.12 shows the results of the case where rigidities of only the roofs, k_r , are increased to ten times of shear stiffness k_s . Furthermore, Fig.13 shows the results of the case where rigidities of bases and roofs,



k_b and k_r , are estimated based on structural properties estimated from the drawing. The rigidity of each floor is calculated with Eq. (8) and Eq. (9).

$$k_b = EA_B/0.5L \quad (8)$$

$$k_r = EA_S/0.5L \quad (9)$$

Where, E : Young's modulus of concrete (2.27×10^7 kN/m²), L : length of the building (65.7m), and A_B and A_S : section area of foundation and superstructure respectively which are shown in Fig.(14).

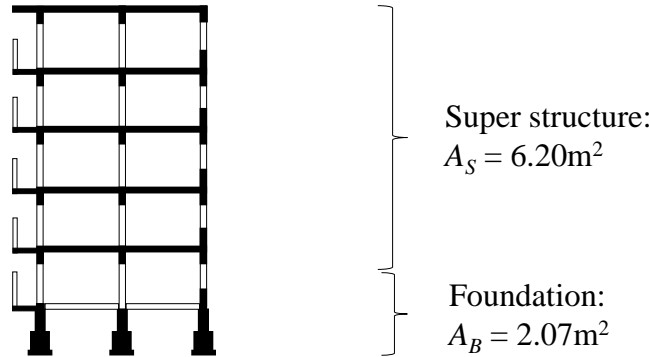


Fig.14 - Section area of structures

We can summarize the analysis results as follows,

- 1) Noises do not appear on the Fourier spectral ratios when floor rigidities are set to about 0.0 (See Fig. 10). Conversely, when floors have some rigidities, noises could appear on the Fourier spectral ratio because input ground motion at a distance from a certain point also affect the behavior of the structure at that point due to an effect of floor rigidity. Then coherence between input ground motions and response of structure would become lower.
- 2) When floor rigidities of a foundation are extremely large, no noise appears on the Fourier spectral ratio of RF/1F (See Fig. 11). We can presume that floor rigidities of foundation cancel out phase differences between input ground motions.
- 3) When floor rigidities of the foundation are relatively small, noises appear on the Fourier spectral ratios of RF/1F, too (See Fig.12 and Fig.13). Noise aspects on the Fourier spectral ratios of the target building structure can be simulated with this type of the model.

4. Evaluation of Signal Power Ratio and Transfer Function

Ikeura clarified that coherence can be expressed by the following equation [7].

$$coh^2(f) = p_{xx}(f)p_{yy}(f) \quad (10)$$

Where, $p_{xx}(f)$ or $p_{yy}(f)$: signal power ratio calculated with the following equation.

$$p_{xx}(f) = D_{xx}(f)/C_{xx}(f) \quad (11)$$

Where, $D_{xx}(f)$: power spectrum of signal component included in $C_{xx}(f)$

If we have records observed at more than three points and calculate more than three coherences, we can evaluate the signal power ratio of each record based on Eq. (10) [7]. Also, we can evaluate transfer functions using the signal power ratio with Eq. (12) [7].

$$H_{xy}(f) = C_{xy}(f) / p_{yy}(f) C_{yy}(f) \quad (12)$$

We apply the Ikeura's method mentioned above to microtremor observation records. We calculate coherences for all combinations of observation records to evaluate the signal power ratios. Fig.15 shows a part of calculation results of coherences. Fig.16 shows the signal power ratios of observation records at GL(1), 1F(4) and RF(7). The signal power ratio of the record on GL becomes almost zero in a frequency range higher than 3Hz; those on 1F and RF become almost zero in a frequency range higher than about 5Hz. Fig.17 shows the transfer functions by Eq. (12). Comparing it with the Fourier spectral ratios shown in Fig.3, peaks may be more distinct in Fig.17. However, they do not reflect vibration characteristics of the target building structure necessarily. Although we need adequate signal components in the frequency range higher than about 2Hz to evaluate vibration characteristics of it, there may be no sufficient signal components in this range as shown in Fig.16 in the case of the microtremor observation.

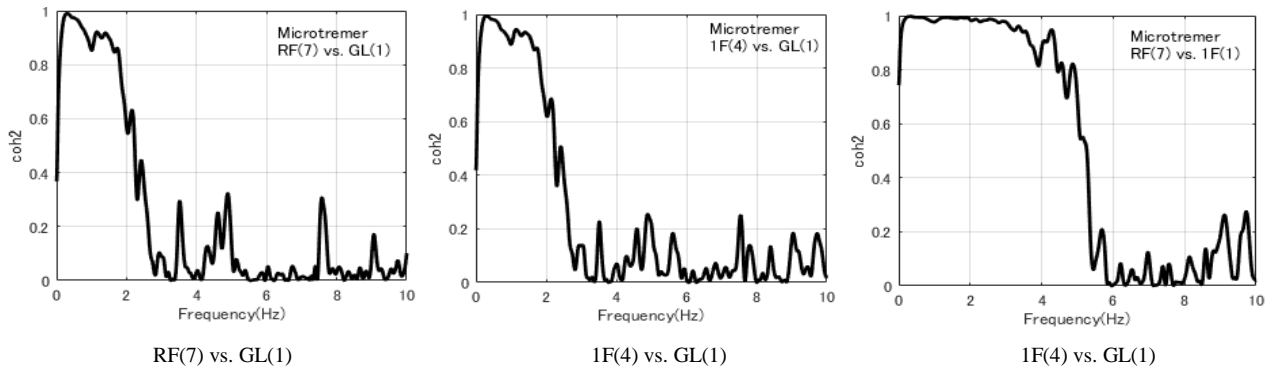


Fig.15 –Coherence, coh^2 , of microtremor records (GL(1), 1F(4), 5F(7))

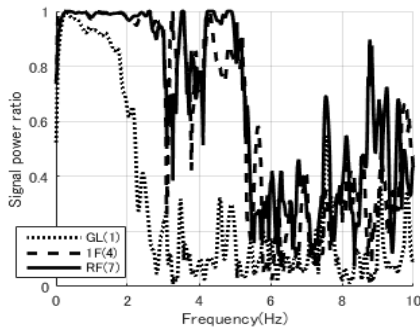


Fig.16 -Signal power ratio of microtremors

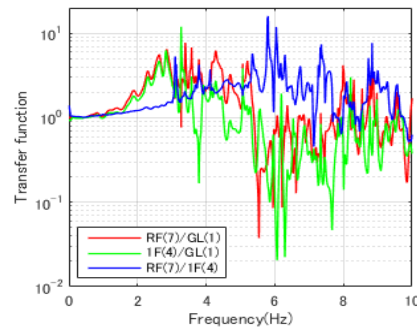


Fig.17 - Transfer function by microtremor records

Figs.18-20 show analysis results of strong motion observation records. As shown in Fig.19, sufficient signal components are acquired, especially in the record at 5F(5). And Fig.20 shows that the transfer functions by Eq. (13) reflect vibration characteristics of the target building more appropriately.

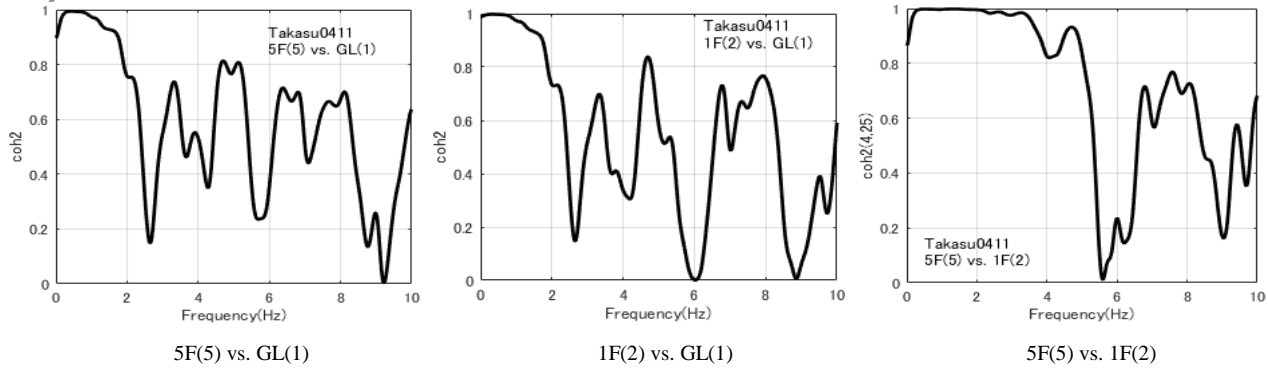


Fig.18 –Coherence, coh^2 , of strong motion observation records (GL(1), 1F(2), 5F(5))

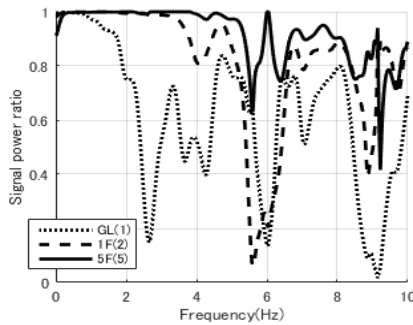


Fig.19 -Signal power ratios of strong motions

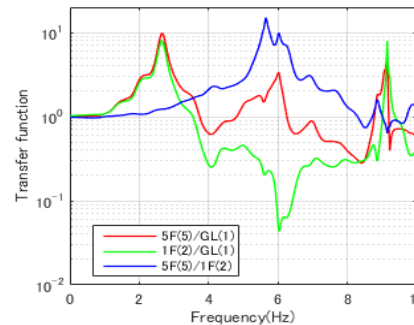


Fig.20 - Transfer function by strong motion records

In the case of strong motion observation, we observe ground motion at only one point as shown in Fig.5. To estimate ground motions X_g at the multi-points, we derive Eq. (13) from Eq. (2) and Eq. (3). For X_s and X_b , we can use strong motion observation records in the building.

$$X_g = [K_{soil}]^{-1} \left\{ ([K_{bs}] + i\omega [C_{bs}]) X_s + (-\omega^2 M_{bb} + [K_{bb}] + i\omega [C_{bb}]) X_b \right\} \quad (13)$$

We can solve this equation with the least squares method. Fig.21 shows the estimated coherence of ground motions at GL(1) and GL(3) shown in Fig.1 for the numerical model of the case 4 ($k_b=1.096k_s$, $k_r=3.281k_s$).

The coherence shown in this figure is higher than that shown in Fig.4 for the microtremor observation records. However, this result suggests there may be some phase differences in the ground motions even in the case of the strong motion observation. We think this result can be one of the sources generate some noises appearing on the Fourier spectral ratios.

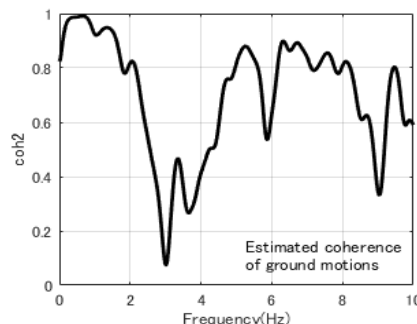


Fig.21 - Estimated coherence, coh^2 , of ground motions on the points, GL(1) and GL(3) in Fig.1



5. Conclusions

We investigated characteristics and generation factors of noises included in the records of microtremor and strong motion observation conducted on the five-story apartment building and the surrounding ground. Conclusions obtained from this study are summarized as follows;

- (1) In the case of microtremor observation records, a coherence of ground motions observed near the both edges of the building structure, of which distance is 65.7m, became about zero in the frequency range higher than 2Hz. It means that there are large phase differences in this range. When the building structure is subjected to ground motions with large phase differences like this, a flexible floor of the foundation generates larger noises on the Fourier spectral ratio of RF/1F as well as other Fourier spectral ratios.
- (2) The signal power ratios of the strong motion observation records became higher than those of the microtremor observation records. Also, the record in the superstructure showed higher signal power ratios than those of ground in the wide frequency range. Transfer function evaluated using signal power ratio for strong motion revealed vibration characteristics of the target building more appropriately.

6. Acknowledgement

This study was conducted as part of the research and development project “Development of Building Seismic Performance Evaluation Technologies in Response to the Advance of Earthquake Motion Information” (FY2011-2014) by the Ministry of Land, Infrastructure, Transport and Tourism (MLIT). We would like to thank staffs of Urban Renaissance Agency and Toda Corporation for their supports to microtremor observations and strong motion observations in this study.

7. References

- [1] SAFAK E (1995): Detection and Identification of Soil-Structure Interaction in Buildings from Vibration Recordings, *Journal of Structural Engineering*, Vol. 121, No.5, ASCE, 899-906.
- [2] STEWART JP, FENVES GL (1998): System Identification for Evaluating Soil-Structure Interacting Effects in Buildings from Strong Motion Records, *Earthquake Engineering and Structural Dynamics*, Vol. 27, 869-885.
- [3] TRIFUNAC MD, IVANOVIC SS, TODOROVSKA MI (2001): Apparent Periods of a Building. I: Fourier Analysis, *Journal of Structural Engineering*, Vol. 127, No. 5, ASCE, 517-526
- [4] HARAGUCHI K, KANDA J, INAGAKI M (2003): A Method for Identification of Multistoried Buildings Considering Soil- Structure Interaction by Microtremor Observation, *J. Struct. Constr. Eng., AIJ*, No. 564, 31-37. (In Japanese)
- [5] KOJIMA H, FUKUWA N, TOBITA J (2005): A Study on Input Loss Effect of Low and Medium Rise Buildings Based on Seismic Observation and Microtremor Measurement, *J. Struct. Constr. Eng., AIJ*, No. 587, 77-84. (In Japanese)
- [6] OKANO H, AZUHATA T, INOUE N, IIBA M, KASHIMA T and SAKO Y (2014): Reduction effect of building structure response by dynamic soil-structure interaction evaluated from observed strong motion, *J. Struct. Constr. Eng., AIJ*, Vol. 79 No.696, 237-246. (In Japanese)
- [7] IKEURA T (2009): Ground transfer functions of seismic waves propagating between vertical array measurement points, *J. JAEE*, Vol.9, No.1, 65-82. (In Japanese)